Gas Permeation and Diffusion in Cross-Linked Poly(ethylene glycol diacrylate)

Haiqing Lin[†,‡] and Benny D. Freeman*[,†]

Department of Chemical Engineering and Center for Energy and Environmental Resources, University of Texas at Austin, Austin, Texas 78758

Received July 29, 2005; Revised Manuscript Received March 5, 2006

ABSTRACT: The permeability of cross-linked poly(ethylene glycol diacrylate) (XLPEGDA) to He, H_2, O_2, N_2, CO_2, CH_4, C_2H_4, C_2H_6, C_3H_6, and C_3H_8 was determined at temperatures ranging from −20 to +45 °C and at fugacities up to approximately 15 atm for some gases. Diffusion coefficients of CO_2 and hydrocarbons were calculated as a function of temperature and local penetrant concentration. The effect of temperature and fugacity on permeability and diffusivity is satisfactorily described using either an activated diffusion model or a free volume-based model.

Introduction

The removal of acid gases (such as CO_2) from nonpolar gases such as CH_4, H_2, and N_2 is important in existing industrial applications and potential future applications.[1] CH_4 is a basic chemical and energy source that is often contaminated with impurities such as CO_2, which must be removed to meet natural gas pipeline specifications.[1] H_2 is a basic chemical that has been proposed as an energy carrier for fuel cells, and current H_2 production via hydrocarbon reforming yields CO_2/H_2 mixtures.[2,3]

Poly(ethylene oxide) (PEO) containing materials have attracted significant attention for the separation of acid gases from mixtures with nonpolar gases.[4−19] Because pure PEO is semicrystalline, and crystallinity should significantly decrease gas permeability, many strategies have been explored to prepare amorphous polymers containing PEO.[8,9] In the first paper of this series, a family of cross-linked poly(ethylene glycol diacrylate) (XLPEGDA) with systematically varying cross-linking density was prepared.[20] Cross-linking was shown to successfully disrupt PEO crystallization with little effect on gas permeability and diffusivity.[20] Furthermore, the effect of fugacity (from 0 to 10 atm) and temperature (from −20 to 35 °C) on gas solubility in cross-linked poly(ethylene glycol diacrylate) (XLPEGDA) was reported.[21] The polar PEO units exhibit favorable interactions with CO_2, leading to high solubility selectivity for CO_2/nonpolar gas pairs. Such interactions become stronger at lower temperatures, which contributes to higher selectivities at lower temperatures.[21]

This paper reports permeability of XLPEGDA to a variety of penetrants (e.g., He, H_2, N_2, O_2, CH_4, CO_2, C_2H_6, C_2H_4, C_3H_8, and C_3H_6) as a function of temperature and penetrant fugacity. These permeability results are combined with gas solubility data to calculate diffusion coefficients as a function of temperature and fugacity. The effect of temperature and fugacity on gas permeability and diffusivity is interpreted using an activated diffusion model and a free volume model.

* Corresponding author. E-mail: freeman@che.utexas.edu. Telephone: +01-512-232-2803. Fax: +01-512-232-2807.

† Department of Chemical Engineering and Center for Energy and Environmental Resources, University of Texas at Austin.

‡ Current address: Membrane Technology and Research, Inc, 1360 Willow Road, Suite 103, Menlo Park, CA 94025.

Background

The permeability of a polymer to a gas A, P_A, is:[22]

$$P_A \equiv \frac{N_A \cdot l}{f_2 - f_1} \tag{1}$$

where N_A is the steady-state gas flux through the film, l is the film thickness, and f_2 and f_1 are the upstream (i.e., high) and downstream (i.e., low) fugacities of gas A, respectively. This definition of permeability uses fugacity instead of pressure to account for nonideal behavior in the gas phase. Some of the more condensable penetrants considered in this study exhibit significant deviations from ideal gas behavior, particularly at low temperature and high pressure, so the use of fugacity is warranted.[21] The fugacity was calculated from the virial equation of state with parameters available in the literature.[21] Permeability coefficients are commonly expressed in Barrers, where 1 Barrer $= 10^{-10}$ cm^3(STP) cm/(cm^2 s cm Hg). If the diffusion process obeys Fick's law and the downstream fugacity is much less than the upstream fugacity, which are believed to be true in this study, the permeability is given by:[23]

$$P_A = D_A \times S_A \tag{2}$$

where S_A is the solubility coefficient, which is also based on fugacity,[21] and D_A is the average effective diffusivity through the film, which is defined by:

$$D_A = \frac{1}{C_2 - C_1}\int_{C_1}^{C_2} \frac{D_{loc}}{1 - w_2}\,dC = \frac{1}{C_2 - C_1}\int_{C_1}^{C_2} D_{eff}\,dC \tag{3}$$

where D_{loc} is the local concentration-dependent diffusion coefficient, C_2 and C_1 are the dissolved penetrant concentrations at the upstream and downstream faces of the polymer, respectively, w_2 is the penetrant mass fraction in the polymer, and D_{eff} is the local effective diffusion coefficient that characterizes the penetrant mobility in the polymer.

As discussed previously,[21] gas sorption in rubbery polymers is often described using the Flory−Huggins model:

$$\ln\frac{f}{f_{sat}} = \ln \phi_2 + (1 - \phi_2) + \chi(1 - \phi_2)^2 \tag{4}$$

10.1021/ma051686o CCC: $33.50
Published on Web 04/14/2006

where f_{sat} is the penetrant saturation fugacity at the temperature of interest, ϕ_2 is the volume fraction of penetrant dissolved in the polymer, and χ is the Flory−Huggins interaction parameter, which is often empirically related to ϕ_2 as follows:[24]

$$\chi = \chi_0 + \frac{\chi_1}{T} + \chi_2(1 - \phi_2) \tag{5}$$

where ϕ_2 is given by:

$$\phi_2 = \frac{C\bar{V}_2}{1 + C\bar{V}_2} \tag{6}$$

and $\bar{V}_2$ is the partial molar volume of the penetrant in the polymer.

Conventionally, local effective diffusion coefficients, D_{eff}, can be derived from eqs 1−3:[25]

$$D_{eff}(C_2) = \left[P_A + f\frac{dP_A}{df}\right]_{f_2}\left(\frac{df}{dC_2}\right)_{f_2} \tag{7}$$

Gas permeability is often empirically related to fugacity as follows:[26]

$$P_A = P_{A,o}\exp(m\Delta f) = P_{A,o}\exp(mf_2) \tag{8}$$

where $P_{A,o}$ is the permeability coefficient when $\Delta f = 0$ (this limit is often achieved by extrapolating to conditions where both f_1 and f_2 are zero, so $P_{A,o}$ is often referred to as the infinite dilution permeability), m is an adjustable constant at a given temperature, and Δf is the difference between the upstream and downstream fugacity: $\Delta f = f_2 - f_1$. In this study, because the downstream fugacity, f_1, is practically 0, Δf is replaced by f_2.

Substituting eqs 4 and 8 into eq 7 yields the following result:

$$D_{eff}(C_2) = P_{A,o}\exp(mf_2)\left(1 + mf_2\frac{f_2}{C_2}\phi_2(1-\phi_2)^2\left[\frac{1}{\phi_2} - 2\chi_0 - \frac{2\chi_1}{T} - 3\chi_2(1-\phi_2)\right]\right) \tag{9}$$

This approach has been used to estimate diffusion coefficients as a function of temperature and penetrant concentration.[8,27] However, it requires values of $P_{A,o}$ and m for each gas at each temperature of interest. This approach leads to a large number of empirical parameters to characterize permeability and diffusivity in a material.

In the absence of penetrant concentration effect, the effect of temperature on gas permeability, solubility, and diffusivity is often described using the Van't Hoff−Arrhenius approach:[28]

$$P_A = P_{A0}\exp\left(\frac{-E_P}{RT}\right) \tag{10}$$

$$S_A = S_{A0}\exp\left(\frac{-\Delta H_S}{RT}\right) \tag{11}$$

$$D_A = D_{A0}\exp\left(\frac{-E_D}{RT}\right) \tag{12}$$

where P_{A0}, S_{A0}, and D_{A0} are preexponential factors, R is the ideal gas constant, T is absolute temperature, and E_P, ΔH_S, and E_D are the activation energy of permeation, enthalpy of sorption, and activation energy of diffusion, respectively. From eqs 10−12, the following expression can be obtained:

$$E_P = E_D + \Delta H_S \tag{13}$$

However, this approach offers no specific prescription for interpreting experimental results when ΔH_S and E_D are functions of penetrant concentration. For these cases, which are often encountered when considering strongly sorbing components in the polymer, we use the recent activated-state diffusion model developed by Prabhakar et al.[29] to interpret the results. In this model, D_{eff}, rather than D_A, is used in eq 12. The concentration and temperature dependence of diffusivity could also be described by a free volume model.

Experimental Section

Materials. Gas cylinders of methane, ethane, ethylene, propane, and propylene of chemical purity (99%) were received from Air Liquide American Corporation (Houston, TX), and 99.9% pure helium, hydrogen, oxygen, nitrogen, and carbon dioxide were purchased from Air Gas Southwest Inc. (Corpus Christi, TX). All gases were used as received. Poly(ethylene glycol) diacrylate ($CH_2{=}CHCOO(CH_2CH_2O)_nOCCH{=}CH_2$, $n = 14$; MW = 743) and 1-hydroxylcyclohexyl phenyl ketone (HCPK) were purchased from Aldrich Chemical Co. (Milwaukee, WI). All chemicals were used as received unless otherwise noted. Ultrapure water was produced by a Milli-Q water purification system (Millipore Corporation, Bedford, MA).

Polymer Synthesis and Film Preparation. The polymer was synthesized from a cross-linker, poly(ethylene glycol) diacrylate, using UV photopolymerization in the presence of 20 wt % water, which acts as an inert solvent. The details regarding the preparation and physical characterization of these materials are discussed elsewhere.[20,21]

Permeation Measurements. The pure gas permeation properties were determined using a constant volume/variable pressure apparatus, which is described elsewhere.[8,30] Polymer samples were partially masked by using impermeable aluminum tape on the upstream and downstream faces.[8,31] Additionally, the leak rate in the system was always measured before starting the permeation experiments, and afterward, the pressure increase in the downstream volume was recorded to determine permeability. Gas permeability was calculated from the steady-state rate of pressure increase in a fixed downstream volume:[8,32]

$$P_A = \frac{V_d l}{f_2 A_m RT}\left[\left(\frac{dp_1}{dt}\right)_{ss} - \left(\frac{dp_1}{dt}\right)_{leak}\right] \tag{14}$$

where V_d is the downstream volume, l is the film thickness, A_m is the film area available for gas transport, R is the gas constant, and $(dp_1/dt)_{ss}$ and $(dp_1/dt)_{leak}$ are the steady-state rates of pressure rise in the downstream volume at a fixed upstream pressure and under vacuum, respectively. $(dp_1/dt)_{leak}$ was usually less than 10% of $(dp_1/dt)_{ss}$. The downstream pressure was always less than 2 cm Hg, which was very low compared with the lowest upstream pressure considered (2 atm). Care was taken to ensure that gas permeation had reached steady state, especially at lower temperatures. After allowing the pressure to rise for about 5 h in the downstream volume, the downstream volume was evacuated and the pressure rise rate was remeasured. The flux was presumed to be at steady state when the last measured flux value was the same as the previous one. In all cases, the measurements were made well after the time since the beginning of the experiment was greater than l^2/D_A, which is within the steady-state regime for gas diffusion according to Fick's law.[33] For example, C_3H_8 permeability at −10 °C was calculated by using the flux measured after 7 days of applying C_3H_8 to the upstream face of the membrane.

The uncertainty in the experimental permeability coefficients was estimated by using a standard propagation of error analysis,[34] and typically, the uncertainty was less than 10%. Gas permeability coefficients were measured with different samples and different

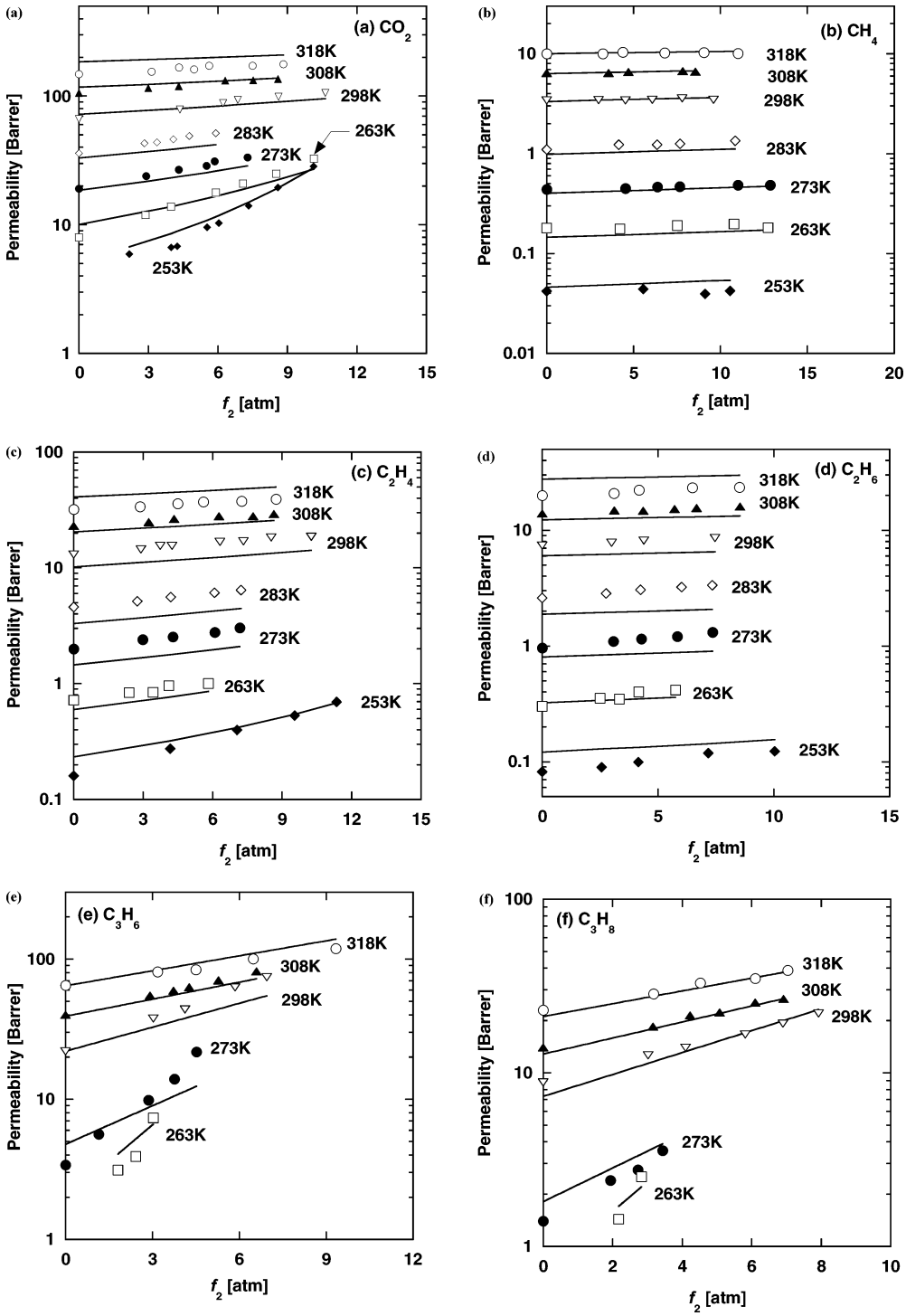

Figure 1. Effect of temperature and fugacity on permeability in XLPEGDA. The lines and curves represent model fits to the experimental data using eq 20 and the adjustable constants in Table 4. The permeability coefficient values at infinite dilution are estimated by using eq 8.

permeation equipment, and the differences among the various permeability coefficients were less than 10%.

Results and Discussion

Permeability. Parts a−f of Figure 1 present permeability coefficients of various gases as a function of temperature and upstream gas fugacity (i.e., f_2) in XLPEGDA. In general, for low-sorbing penetrants, such as the permanent gases (He, H_2, N_2, O_2, and CH_4) over the entire temperature range considered (i.e., −20 to 45 °C) and C_2H_6 at temperatures higher than 10 °C, permeability coefficients are essentially independent of f_2. The permeability coefficients of He, H_2, N_2, and O_2 are not shown here for brevity. In contrast, the permeability coefficients of highly sorbing penetrants, such as CO_2, C_3H_8, and C_3H_6, increase with increasing f_2, especially at lower temperatures. For example, at −20 °C, CO_2 permeability increases by almost 400%, from 5.9 to 28 Barrers, as f_2 increases from 2.2 to 10.1 atm. This behavior is consistent with permeation properties of rubbery polymers.[27] Polymers can sorb significant amounts of a diluent such as CO_2 or C_3H_8, leading to a decrease in polymer glass transition temperature and, in turn, an increase in polymer chain flexibility and fractional free volume, thereby increasing gas diffusion coefficients and permeability coefficients.[35] Additionally, solubility typically increases with increasing fugacity

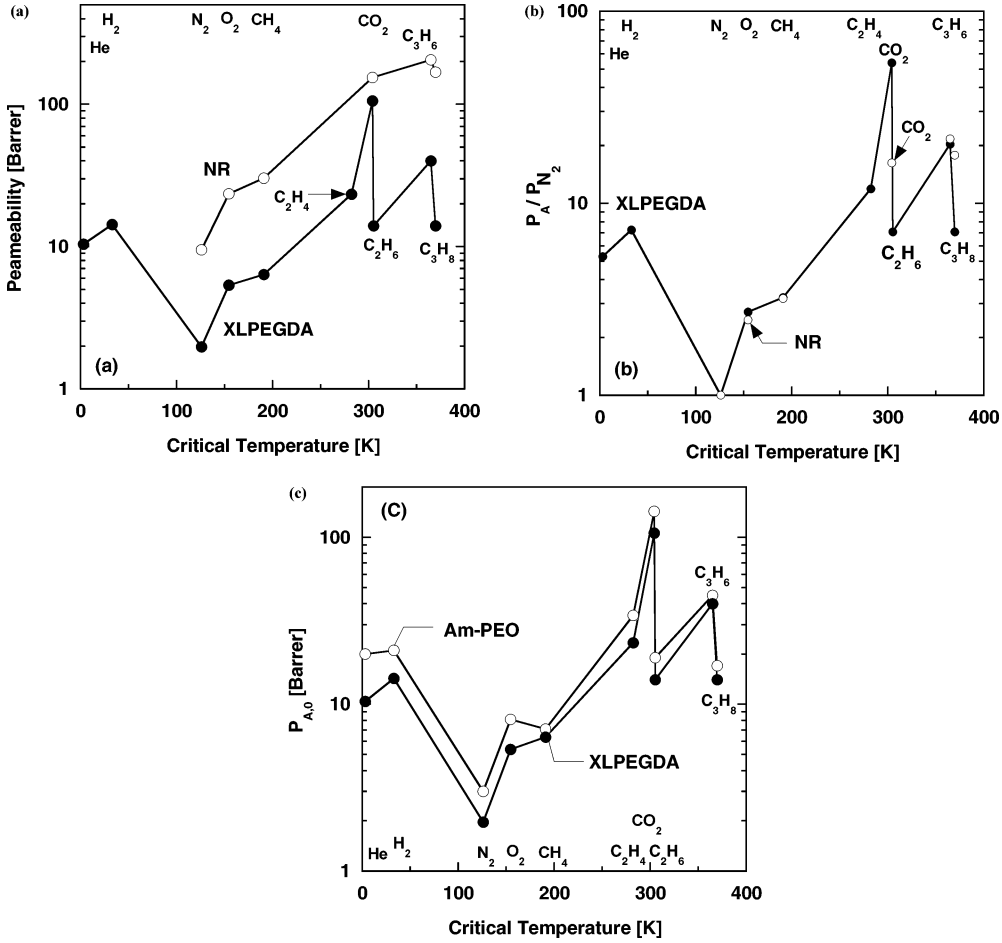

Figure 2. Effect of penetrant critical temperature on (a) infinite dilution permeability in XLPEGDA at 35 °C (●) and natural rubber (NR) at 25 °C[37] (○); (b) permeability selectivity over N_2 at infinite dilution; (c) infinite dilution permeability in XLPEGDA and amorphous poly(ethylene oxide) (Am-PEO) at 35 °C.[8] The line in Figure 2b connects the selectivity values of XLPEGDA.

in rubbers,[21] and this factor also acts to increase permeability coefficients at higher fugacity.[36] These effects will be quantitatively discussed later in this paper.

Equation 8 was used to characterize the effect of fugacity on permeability coefficients and to estimate infinite dilution permeability coefficients (i.e., $P_{A,o}$). The $P_{A,o}$ values estimated by this approach are presented in the figures (except for C_3H_6 and C_3H_8 at −10 °C). For C_3H_6 and C_3H_8 at −10 °C, the small number of data points and the strong sensitivity of permeability to fugacity made extrapolation using such an empirical model risky. The fitting constants for this empirical model are not shown here for brevity, and the lines in Figure 1 represent fits of a model discussed later. To illustrate the relative magnitude of permeability coefficients among these penetrants, Figure 2a presents $P_{A,o}$ as a function of penetrant critical temperature at 308 K. The infinite dilution permeability coefficients are used for comparison to minimize the effect of penetrant concentration on permeability.[27] In the temperature ranges studied, $P_{A,o}$ values decrease in the following order:

$$CO_2 > C_3H_6 > C_2H_4 > H_2 \approx He > C_3H_8 \approx C_2H_6 > CH_4 \approx O_2 > N_2$$

This is the same order as that observed in semicrystalline PEO.[8] Generally, penetrants with higher critical temperature are more condensable and, therefore, more soluble. However, more condensable penetrants are often larger and, therefore, exhibit lower diffusion coefficients.[23] Permeability reflects the tradeoff between these often conflicting contributions from solubility and diffusivity. In rubbery polymers, solubility selectivity typically dominates permeability selectivity, and in some cases, larger penetrants such as C_3H_8 can exhibit higher permeability than smaller penetrants such as N_2 and O_2, as illustrated in Figure 2a for gas transport in natural rubber (NR) at 25 °C.[37] Such effects can become more significant if a penetrant has favorable interactions with the polymer. For example, CO_2 enjoys favorable interactions with XLPEGDA,[21] and not surprisingly, CO_2 is the most permeable penetrant in this study. In nonpolar NR, CO_2 does not exhibit specific interactions with the polymer. As a result, CO_2 permeability in NR is consistent with its critical temperature (T_c) rather than being much higher than its T_c value would suggest, which is the case for XLPEGDA. For He and H_2, which are the smallest gases considered, diffusion coefficients are presumably high enough that their permeability coefficients are larger than those of several more condensable penetrants such as O_2 and N_2. Olefins exhibit higher permeability than their corresponding paraffins due to the favorable interactions between the double bonds in the olefins and the polar ether oxygen in the polymer, leading to higher olefin solubility than paraffin solubility.[8,21] Figure 2b presents the effect of critical temperature on penetrant selectivity over N_2 at infinite dilution in XLPEGDA at 35 °C and NR at 25 °C. The selectivity values in NR are near those of XLPEGDA, except for CO_2/N_2. XLPEGDA exhibits much higher CO_2/N_2 selectivity than NR due to the specific interactions between XLPEGDA and CO_2.

Recently, gas permeability properties have been reported for semicrystalline PEO.[8] By using a simple two-phase model (i.e.,

Table 1. Permeation, Diffusion, and Sorption Properties at Infinite Dilution in XLPEGDA[a]

	permeability			diffusivity			solubility		
gas	temperature range	$P_{A0} \times 10^{-8}$	E_P	temperature range	$D_{A0} \times 10^{-3}$	E_D	temperature range	$S_{A0} \times 10^3$	ΔH_S
He	25/45	0.043 ± 0.005	33 ± 2						
H_2	−20/45	2.6 ± 0.3	43 ± 1						
N_2	−20/45	120 ± 10	57 ± 1						
O_2	−20/45	43 ± 3	52 ± 1						
CH_4	−20/45	190 ± 20	56 ± 1	−20/35	1.5 ± 0.3	57 ± 2	−20/35	95 ± 15	-1 ± 1
CO_2	−20/45	4.6 ± 0.5	39 ± 1	−20/35	1.8 ± 0.2	56 ± 1	−20/35	1.9 ± 0.1	-17 ± 1
C_2H_4	−20/45	310 ± 40	54 ± 1	−20/35	7 ± 1	61 ± 2	−20/35	34 ± 4	-7.5 ± 0.4
C_2H_6	−20/45	620 ± 60	57 ± 1	−20/35	11.6 ± 1.4	63 ± 2	−20/35	41 ± 3	-6.4 ± 0.3
C_3H_6	0/45	580 ± 60	54 ± 2	0/35	32 ± 6	67 ± 3	−10/35	14 ± 2	-13 ± 1
C_3H_8	0/45	440 ± 60	56 ± 2	0/35	12 ± 2	65 ± 3	−20/35	29 ± 4	-9.4 ± 0.3

[a] E_D is calculated as $E_p - \Delta H_S$, and D_{A0} is calculated as P_{A0}/S_{A0}. The units for temperature, P_{A0}, D_{A0}, and S_{A0} are °C, Barrer, cm^2/s, and $cm^3(STP)/(cm^3$ atm), respectively. The units for E_D, E_P, and ΔH_S are kJ/mol.

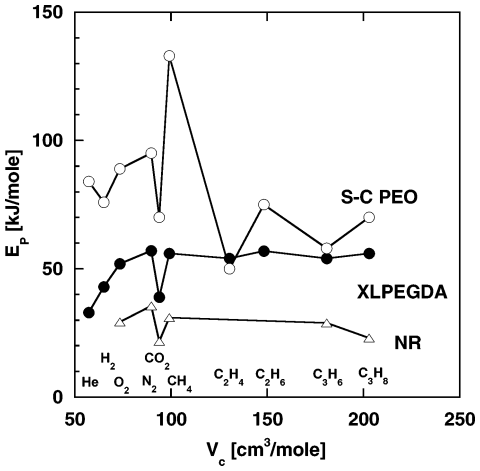

Figure 3. Activation energy of permeation at infinite dilution as a function of penetrant critical volume in XLPEGDA, natural rubber (NR),[37] and semicrystalline poly(ethylene oxide) (S-C PEO).[8]

assuming that the crystalline phase is not accessible to penetrant sorption or diffusion and only increase the penetrant diffusion path without immobilizing the amorphous phase polymer chains[8,37,38]), permeability coefficients in wholly amorphous poly(ethylene oxide) (Am-PEO) can be estimated.[8] These estimated values are reported in Figure 2c and compared with those in XLPEGDA. The estimated permeability coefficients in Am-PEO are quite close to those in XLPEGDA, which is gratifying given the strong approximations in the two-phase model used to make the extrapolation required for Am-PEO and the fact that XLPEGDA is only about 82 wt % PEO (the remainder of the XLPEGDA structure is ethyl ester linkages).

The temperature dependence of infinite dilution permeability coefficients in XLPEGDA can be modeled by using eq 10. The values of P_{A0} and E_P at infinite dilution are recorded in Table 1 and are presented in Figure 3. With the exception of CO_2, as penetrant size increases, E_P values increase and then level off, presumably reflecting the interplay between E_D (which increases with increasing penetrant size) and ΔH_S (which often decreases with increasing penetrant size). Figure 3 compares E_P values in XLPEGDA with those in natural rubber (NR)[37] and semicrystalline poly(ethylene oxide) (S-C PEO).[8] NR is an amorphous hydrocarbon polymer, and as such, it provides a useful point of comparison for XLPEGDA. Because XLPEGDA contains polar groups, it has lower free volume and higher cohesive energy density than NR;[8,21] both of these factors can increase barriers to diffusion.[8] Consequently, E_P values in XLPEGDA are higher than those in NR despite the fact that the dependence of E_p on T_c is very similar in these polymers. Interestingly, E_p values for larger penetrants, such as C_2H_4 and C_3H_6, are quite similar in semicrystalline PEO and XLPEGDA, but E_p values for smaller penetrants, like O_2 and CH_4, in semicrystalline PEO are much larger than those in XLPEGDA. The effect of crystal morphology and crystalline constraints on the mobility of the amorphous material might play a role in determining E_p values in S-C PEO; however, these effects are not well-understood at a molecular level.[37]

Diffusivity. Parts a−f of Figure 4 present the calculated results of $D_{eff}(C_2)$ as a function of penetrant concentration and temperature for various gases using eq 9, including D_{eff}^{∞}, the diffusion coefficient at infinite dilution. Over the temperature range considered in this study, D_{eff}^{∞} decreases in the following order:

$$CO_2 > CH_4 > C_2H_4 > C_2H_6 > C_3H_6 > C_3H_8$$

This is the same order as penetrant size characterized by critical volume. The penetrant size dependence of gas diffusion coefficients in polymers has been described by using the following empirical equation:[27,28,39−41]

$$D_{eff}^{\infty} = \frac{\tau}{V_c^{\eta}} \tag{15}$$

where τ and η are adjustable constants. The parameter η characterizes the sensitivity of diffusivity to penetrant size. Larger η values indicate stronger size-sieving ability. As indicated in Figure 5, the data are well described by eq 15, and η values as a function of temperature are recorded in Table 2. As temperature decreases, η values generally increase, indicating an increase in size-sieving ability with decreasing temperature. Typically, decreasing temperature increases polymer chain rigidity, resulting in an increase in size-sieving ability.

Figure 6 compares the dependence of D_{eff}^{∞} on critical volume in XLPEGDA at 35 °C with that in NR at 25 °C,[37] poly(dimethylsiloxane) (PDMS) at 35 °C[27] and semicrystalline PEO (S-C PEO) at 35 °C.[8] The detailed values of η (and τ for XLPEGDA) are recorded in Table 2. On the basis of the η values at 35 °C, XLPEGDA has a size-sieving ability similar to that in PDMS, even though XLPEGDA exhibits much lower diffusion coefficients than PDMS. PDMS has the lowest T_g of all known polymers, and it exhibits very weak size-sieving ability. Interestingly, XLPEGDA also has a size-sieving ability similar to that of NR, although it has been conventionally believed that, due to polar−polar interactions, polar polymers would have higher cohesive energy density and thus stronger size-sieving ability than nonpolar rubbery polymers such as NR. Polar XLPEGDA and nonpolar NR may exhibit similar size-sieving ability due to the flexible nature of the ether oxygen

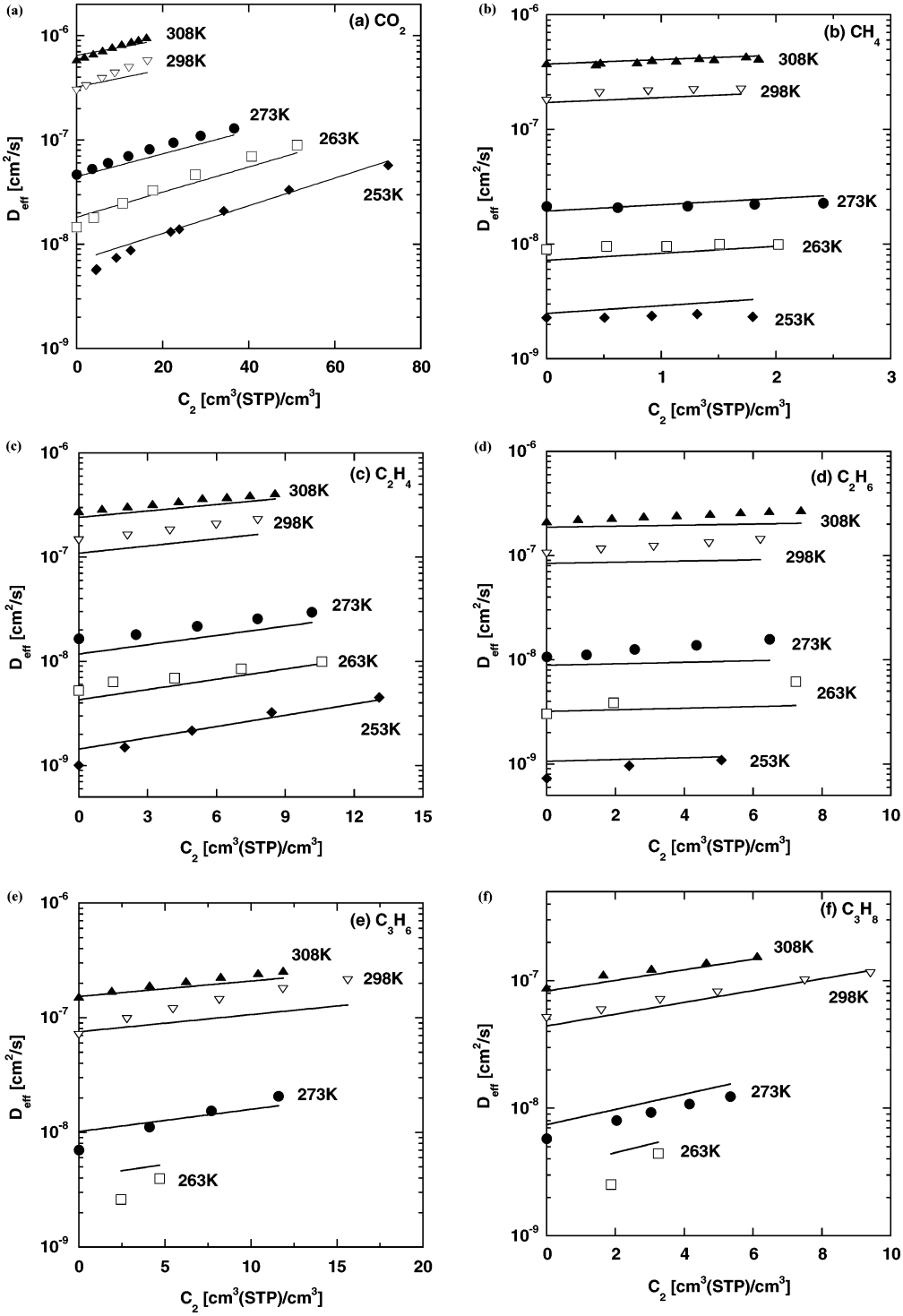

Figure 4. Influence of temperature and concentration on local effective diffusion coefficients. (a) CO_2, (b) CH_4, (C) C_2H_4, (d) C_2H_6, (e) C_3H_6, (f) C_3H_8. The lines and curves are based on eq 18 and the parameters recorded in Table 4. The infinite dilution values were estimated by using eq 9.

linkages in XLPEGDA.[9] We have reviewed the effect of polar groups on gas solubility, diffusivity, permeability, and CO_2/H_2 permeability selecitivity.[9] Generally speaking, the addition of polar groups to a polymer increases polymer cohesive energy density, leading to a decrease in CO_2 diffusion coefficients and CO_2/H_2 selectivity (i.e., an increase in the size-sieving ability). However, ether oxygens are an exception to this rule of thumb.[9] When ether oxygens are inserted in polyethylene (PE) to form poly(ethylene oxide), CO_2 permeability and CO_2/H_2 selectivity increase.[8] The presence of ether oxygens in PEO seems to offer little hindrance to chain mobility. For example, extrapolated T_g values are −89 °C for wholly amorphous PEO and −80 °C for wholly amorphous PE,[42] so PEO chains are as flexible, if not slightly more flexible, than PE chains. Therefore, the polar ether oxygens in XLPEGDA do not necessarily increase polymer chain rigidity and, in turn, size-sieving ability. Semicrystalline PEO seems to have the strongest size-sieving ability among these polymers, probably due to its crystalline nature. To put these values in perspective, η is 10.5 for poly(vinyl chloride) (a very strongly size-sieving glassy polymer)[27] and 0.45 for organic liquids such as hexane and benzene (matrixes with very weak size-sieving ability).[27]

Gas diffusion in nonporous polymers is often interpreted as an activated process described using eq 12. E_D values were

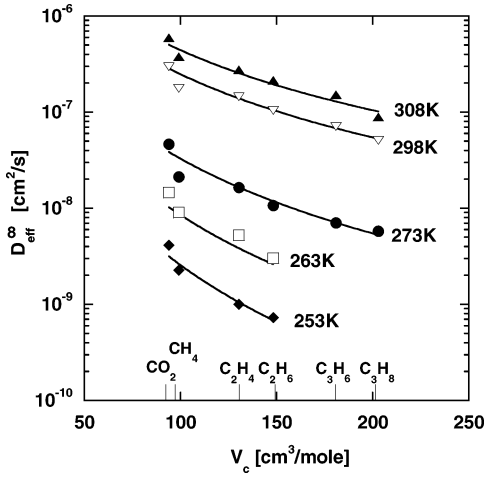

Figure 5. Effect of temperature on the correlation between penetrant critical volume and infinite dilution diffusion coefficients in XLPEGDA.

Table 2. Adjustable Constants for the Correlation between Diffusivity and Penetrant Critical Volume[a]

temperature [K]	η S-C PEO[8]	NR[37]	PDMS[27]	hexane[39]	XLPEGDA	$\tau \times 10^3$ XLPEGDA
308	2.7	2.0	2.3		2.1 ± 0.1	6.4 ± 0.6
298				0.45	2.2 ± 0.1	5.8 ± 0.7
273					2.6 ± 0.1	4.8 ± 0.6
263					3.0 ± 0.1	8.5 ± 0.9
253					3.4 ± 0.1	13 ± 2

[a] S-C PEO: semicrystalline poly(ethylene oxide); NR: natural rubber; PDMS: poly(dimethylsiloxane). τ has units of $cm^2\ cm^{3\eta}/(mole^{\eta}\ s)$.

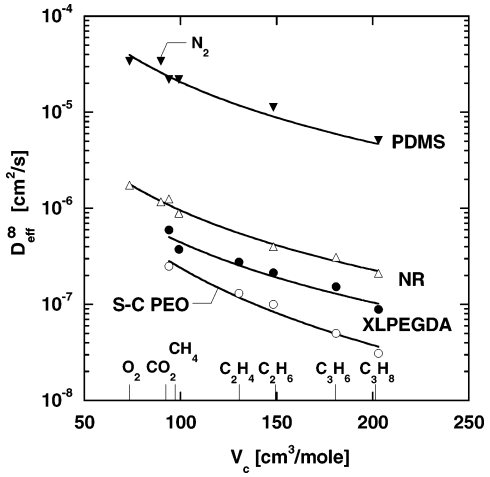

Figure 6. Correlation between penetrant critical volume and infinite dilution diffusion coefficients in XLPEGDA at 35 °C, semicrystalline PEO at 35 °C,[8] PDMS at 35 °C,[27] and NR at 25 °C.[37]

estimated by using eq 13, and D_{A0} values were obtained by using an expression from eqs 10−12, i.e., $D_{A0} = P_{A0}/S_{A0}$. The results (at infinite dilution) are recorded in Table 1. Figure 7 presents E_D values at infinite dilution as a function of Lennard−Jones diameter squared[43] in XLPEGDA, rubbery NR,[37] and the glassy amorphous fluorinated polymer, poly(2,2-bis(trifluoromethyl)-4,5-difluoro-1,3-dioxole-*co*-tetrafluoroethylene) (AF2400).[44] For all polymers, E_D values increase as penetrant size increases. E_D values in XLPEGDA are higher than those in NR, presumably due to the polar nature of XLPEGDA, which leads to lower free volume and higher cohesive energy density.[8] For small penetrants, glassy polymers such as AF2400 exhibit lower E_D values than rubbery polymers because glassy polymers contain

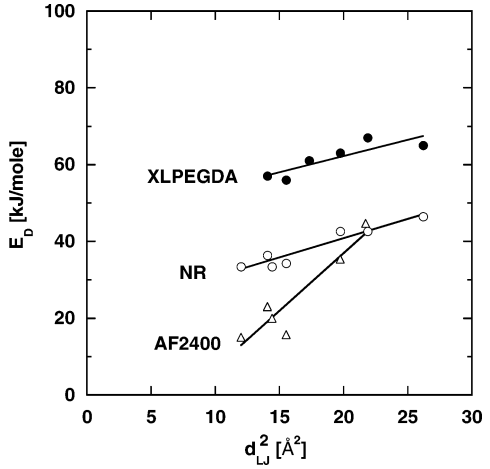

Figure 7. Comparison of activation energy of diffusion values at infinite dilution in rubbery XLPEGDA with those in nonpolar rubbery NR[37] and glassy AF2400.[44] The best fit lines for XLPEGDA, NR, and AF2400 are $E_D = 45(\pm 1) + 0.84(\pm 0.06)\ d_{LJ}^2$, $E_D = 21 + d_{LJ}^2$, $E_D = -23 + 3.0\ d_{LJ}^2$, respectively, when E_D and d_{LJ} have units of kJ/mol and Å, respectively. The values of d_{LJ} are 3.75, 3.94, 4.16, 4.44, 4.68, and 5.12 Å for CH_4, CO_2, C_2H_4, C_2H_6, C_3H_6, and C_3H_8, respectively.[43]

microvoids where the diffusion of small gas molecules requires little polymer segmental motion to open a gap to accommodate the diffusion step of a penetrant molecule. On the other hand, the slope of the best-fit line for AF2400 is much larger than that for the rubbery polymers, indicating that diffusivity in glassy AF2400 is much more sensitive to penetrant size than in the rubbery polymers.[45,46] A low free volume glassy polymer such as polycarbonate would have an even larger slope than that of AF2400.[44−46] In addition to high E_D values, the XLPEGDA and NR data points extrapolate to a positive activation energy at zero penetrant size. However, presumably, E_D values could decrease faster at low d values than expected based on the trend in Figure 7, so it is not possible to draw conclusions about the behavior of this relationship for penetrants smaller than those considered in this study.

In summary, the size-sieving ability of XLPEGDA is rather weak (i.e., similar to that of PDMS and NR), but this is not because E_D values are low for all of the penetrants, which would be consistent with a Meares-type view of the diffusion process if the polymer cohesive energy density were low.[47] Rather, XLPEGDA has higher cohesive energy density (around 19.8 $MPa^{0.5}$)[21] than NR (16.6 $MPa^{0.5}$)[8] and PDMS (15.4 $MPa^{0.5}$).[27] It is weakly size-sieving because E_D values change little from penetrant to penetrant, but the absolute values of E_D are quite high, similar to or higher than those in rigid glassy polymers.[44] This result indicates that the energy required to open a gap in the polymer matrix large enough to permit a penetrant diffusion step is large, but when these gaps are opened, they are sufficiently large to accommodate, with little discrimination, any of the penetrant molecules considered in this study. The molecular origin of this result is not clear.

Figure 8 presents D_{A0} values as a function of E_D/R at infinite dilution, and a simple relationship is observed:[46]

$$\ln D_{A0} = a\frac{E_D}{R} - b \qquad (16)$$

This linear free energy effect describes the so-called compensation effect; that is, higher E_D values are typically accompanied by higher D_{A0} values.[46] This behavior has been observed for other activated processes such as the kinetics of chemical

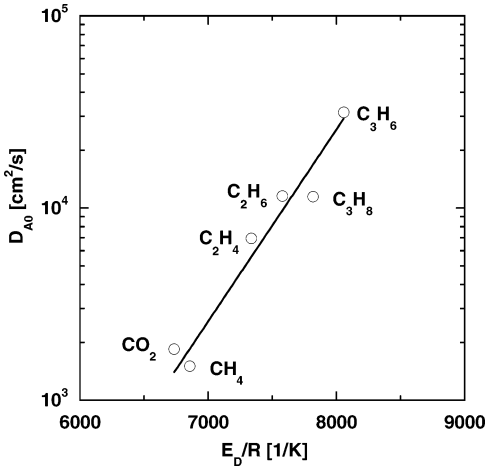

Figure 8. Linear free energy relation between diffusion parameters in XLPEGDA at infinite dilution.

reactions and the viscosity of organic liquids, molten salts, and metals.[45,48] The *a* and *b* values obtained by fitting eq 16 to the diffusion parameters in XLPEGDA are 0.0023 K^{-1} and 8.2, respectively. As shown in Table 3, these values are consistent with the literature data.

In general, the above interpretation of gas permeability and diffusivity relies on eq 8, which empirically relates permeability to fugacity using two temperature-dependent parameters, $P_{A,o}$ and *m*. $P_{A,o}$ at various temperatures can be modeled by using eq 10 and two parameters (i.e., P_{A0} and E_P). However, the dependence of *m* on temperature is unknown, and thus it is impossible to predict permeability and diffusivity unless *m* has been obtained at the temperature of interest. Additionally, the values of *m* might be significant, especially for highly condensable penetrants such as CO_2 and C_3H_8, as illustrated in Figure 1a and f. From this perspective, it would be interesting to explore models with fewer adjustable parameters to describe the dependence of permeability on fugacity. Additionally, there is no simple prescription, beginning from eqs 10−12, to include concentration in the various activation energies in a self-consistent fashion.

Prabhakar et al. Model. Prabhakar and co-workers have described the concentration dependence of diffusivity by using activated-state theory, so the concentration dependence of diffusivity must arise from a concentration dependence of E_D, which is described empirically as follows:[29]

$$E_D = E_D^{o}(1 - kC) \tag{17}$$

where E_D^{o} is the activation energy of diffusion at infinite dilution, and *k* is an adjustable constant, which is independent of temperature. From eqs 2, 3, 12, 16, and 17,[29] the following expressions are obtained:

$$D_{eff}(C_2) = e^{-b} \exp[\alpha E_D^{o} (1 - kC_2)] \tag{18}$$

$$P_A = \frac{e^{-b}}{f_2 - f_1} \frac{\exp[\alpha E_D^{o}(1 - kC_2)] - \exp[\alpha E_D^{o}(1 - kC_1)]}{(-\alpha E_D^{o} k)} \tag{19}$$

where

$$\alpha = \frac{1}{R}\left(a - \frac{1}{T}\right)$$

Because the downstream fugacity is near zero in this study, $f_1 = 0$, $C_1 = 0$, and eq 19 reduces to

$$P_A = \frac{e^{-b}}{f_2} \frac{\exp[\alpha E_D^{o}(1 - kC_2)] - \exp(\alpha E_D^{o})}{(-\alpha E_D^{o} k)} \tag{20}$$

which directly describes the correlation between P_A and f_2; eqs 4−6 relate C_2 to f_2. This approach has been used to model permeability in rubbery polymers such as PDMS and polyethylene (PE) as a function of temperature and penetrant pressure.[29]

This model is applied to gas permeability data in XLPEGDA at a variety of temperatures and fugacities by using nonlinear least-squares fits. These model fits are presented in Figure 1a−f, which, in most cases, describe the experimental data reasonably. The best-fit values of adjustable constants (i.e., E_D^{o}, *b*, and *k*) are recorded in Table 4. χ_0, χ_1, and χ_2 were determined in independent gas solubility experiments; they characterize the temperature and concentration dependence of the Flory−Huggins interaction parameter. These sorption parameters have been reported elsewhere[21] and are recorded in this table for completeness. The value of *a* is set to 0.0023 K^{-1} as suggested by Prabhakar et al.[29] As illustrated in Table 4, the values of *b* for all penetrants are in the range of the literature values in Table 3. However, it was not possible to obtain good fits to the data by using a single, universal value of *b* for all penetrants. It appears that the single value of *b* obtained from fitting the infinite dilution results in Figure 8 to eq 16 does not remain valid when all of the data, at various concentrations, are included in the more general model (i.e., eq 20). This result may also suggest the need for a more critical examination of eq 17 and its ability to describe data over a wide range of conditions and for a variety of penetrants. Except for C_3H_6 and C_3H_8, E_D^{o} values are close to the values of activation energy of diffusion at infinite dilution, as recorded in Table 1.

$D_{eff}(C_2)$ can be also described by this model using eq 18 and the constants in Table 4. As illustrated in Figure 4a−f, the model fits are generally good. This result is encouraging because the increase in gas diffusivity with increasing concentration can be substantial. For example, as concentration increases from 0 to 72 cm^3 (STP)/cm^3 polymer at −20 °C, CO_2 diffusivity increases by more than 1 order of magnitude, from 4.1×10^{-9} to 5.8×10^{-8} cm^2/s.

Table 3. Comparison of Linear Free Energy Correlation Parameters[a]

	polymer	*a* (K^{-1})	*b*
Van Krevelen[46]	rubbers	0.0023	9.2
Barrer & Skirrow[48]	rubbers	0.0019	9.2
Van Amerogen[71]	rubbers	0.0023	8.6/9.7
Prabhakar et al.[29]	PDMS	0.0020	8.3/10.2
This study	XLPEGDA	0.0023 ± 0.0001	8.2 ± 0.2

[a] These values of *b* presume that diffusion coefficients are expressed in units of cm^2/s.

Table 4. Adjustable Parameters for Permeability[a]

constants	CO_2	CH_4	C_2H_4	C_2H_6	C_3H_6	C_3H_8
E_D^{o}	54 ± 1	59 ± 1	60 ± 1	61 ± 1	54 ± 1	48 ± 1
k	2.9 ± 0.4	13 ± 9	6.9 ± 0.3	1.6 ± 1.1	5 ± 1	17 ± 1
b	8.2 ± 0.1	8.1 ± 0.1	8.4 ± 0.1	8.6 ± 0.1	9.5 ± 0.1	10.8 ± 0.1
χ_0	3.7	−3.8	−0.33	1.5	−0.86	−0.89
χ_1	−360	1590	485	750	490	980
χ_2	−1.6	0	0.24	−1.9	0.84	−0.13

[a] Units for E_D^{o}, *k*, and χ_1 are kJ/mol, 10^{-3} cm^3/cm^3(STP), and K, respectively. Values of χ_0, χ_1, and χ_2 are reported elsewhere.[21]

This model relies on an empirical equation, eq 17. However, the value of k in eq 17 cannot be quantitatively predicted. In addition to activated-state theory, free volume models are also often used to interpret gas diffusion in polymers. In the next section, a free volume model is used to describe the effect of penetrant concentration and temperature on diffusivity. This model circumvents the use of eq 17 and the linear free energy relation (i.e., eq 16).

Free Volume Model. Free volume models have been used to describe the influence of the free volume of a polymer/penetrant mixture on penetrant self-diffusion coefficients in polymers.[49−51] The self-diffusion coefficients are related to mutual diffusion coefficients (i.e., D_{loc}) as described in the literature.[50,52] A convenient diffusion coefficient often considered in gas separation membrane studies is the effective diffusion coefficient, D_{eff}; the relation between D_{eff}, D_{self}, and ultimately, free volume, is:[50,53,54]

$$D_{eff} = \frac{Q}{1 - w_2} D_{self} = \frac{Q}{1 - w_2} A_D \exp\left(-\frac{B}{FFV}\right) \qquad (21)$$

where A_D and B are adjustable constants typically taken to be independent of temperature and diluent concentration, Q is a thermodynamic factor, and FFV is the fractional free volume, which is defined as follows:[53]

$$FFV = \frac{V - V_0}{V} \qquad (22)$$

where V is the specific volume of the polymer at the temperature of interest, and V_0 is the specific occupied volume at 0 K. V_0 is estimated as 1.3 times the van der Waals volume of the polymer repeat unit, which is estimated by using a group contribution method.[46]

In the field of gas separation using polymers, penetrant sorption levels are often low, so the value of $Q/(1 - w_2)$ is typically near unity, and in these cases, $D_{eff} = D_{self}$, so correlations are often sought between D_{eff} and FFV.[53,54] This assumption is evaluated as follows. Q can be written as:[52]

$$Q = \frac{C_2}{f_2} \frac{df_2}{dC_2} \qquad (23)$$

Substituting eqs 21 and 23 into eq 7 yields the following result:

$$D_{self} = (1 - w_2)\left[P_A + f\frac{dP_A}{df}\right]_{f2}\frac{f_2}{C_2} = (1 - w_2)P_A\frac{f_2}{C_2}(1 + mf_2) \qquad (24)$$

As an example, Figure 9 presents the values of D_{eff}/D_{self} at various temperatures and fugacities for CO_2. In most cases, D_{eff}/D_{self} values are between 0.85 and 1. Moreover, D_{eff}/D_{self} values for other penetrants at the temperatures and fugacities studied are also in this range. They are not shown here for brevity. Therefore, the difference between D_{eff} and D_{self} is within the uncertainty of D_{eff} (which is, on average, ±15%), and the assumption that $D_{eff} = D_{self}$ is a reasonable approximation for this study. As such, eq 21 becomes

$$D_{eff} = A_D \exp\left(-\frac{B}{FFV}\right) \qquad (25)$$

Equation 25 has been used to correlate the gas diffusion coefficient with fractional free volume in about 40 polymeric materials containing ethylene oxide units (including XLPEGDA).[9] The fractional free volume is related to the glass transition temperature, T_g, of the ethylene oxide components in these polymers by:[9]

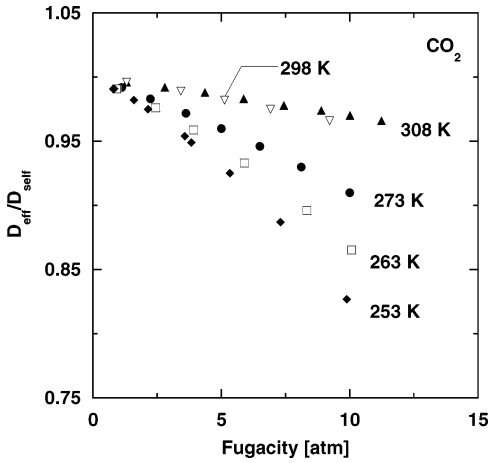

Figure 9. The values of D_{eff}/D_{self} for CO_2 at various fugacities and temperatures.

$$FFV = 0.055 + 8.4 \times 10^{-4}(T - T_g) \qquad (26)$$

where 0.055 is the apparent fractional free volume at T_g, and 8.4×10^{-4} K^{-1} is the apparent expansion coefficient of the fractional free volume, which is similar to the thermal expansion coefficient of low-molar-mass, liquid poly(ethylene oxide) oligomers.[9,55] Equations 25 and 26 can be combined to provide the following model of diffusivity on temperature and diluent concentration, if the effect of diluent concentration on T_g is known:

$$D_{eff} = A_D \exp\left(\frac{-B}{0.055 + 8.4 \times 10^{-4}(T - T_g)}\right) \qquad (27)$$

where A_D and B are adjustable constants for each penetrant that are independent of temperature and concentration, at least to a first approximation.

The presence of a strongly sorbing penetrant in a polymer can swell the polymer matrix, resulting in enhanced segmental mobility and a depression in T_g,[56] which has been widely investigated by experimental measurements[57−60] and theoretical modeling[58,61−64] because of the significant effect of diluents on material properties in polymer processing[58] and membrane separations.[56] Chow developed the following expression to predict the decrease in T_g with increasing diluent concentration in polymer−diluent systems:[61]

$$\ln\frac{T_g}{T_{g0}} = \beta[(1 - \theta)\ln(1 - \theta) + \theta \ln \theta] \qquad (28)$$

where

$$\theta = \frac{M_p}{zM_d}\frac{w_2}{1 - w_2}, \qquad w_2 = \frac{C_2 M_d}{C_2 M_d + \rho_p}, \qquad \text{and } \beta = \frac{zR}{M_p \Delta C_{pp}}$$

Here, T_{g0} and T_g are the glass transition temperatures of pure polymer (i.e., 231 K for XLPEGDA) and the polymer−diluent mixture, respectively, when the diluent weight fraction is w_2. M_p and M_d are the molecular weights of the polymer repeat unit (which is taken as 44 g/mol in this study because this is the molecular weight of an ethylene oxide moiety) and diluent, respectively. ρ_p is the polymer density. ΔC_{pp} is the change in

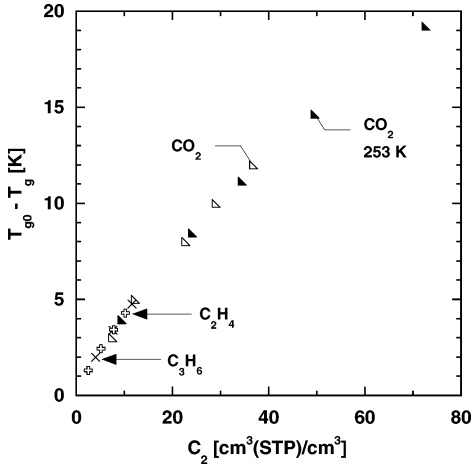

Figure 10. Calculated influence of penetrant concentration on the glass transition temperature of the polymer/gas mixture (T_g). The T_g of pure XLPEGDA, T_{g0}, is 231 K.[20] The calculations correspond to sorption at 273 K, unless otherwise mentioned. Chow's model is used to estimate the influence of gas concentration on T_g.[61]

heat capacity of the pure polymer at its glass transition, 0.99 J/(g °C), which was obtained from differential scanning calorimetry (DSC) experiments on XLPEGDA. This value is consistent with the value reported in the literature for amorphous poly(ethylene oxide) (0.948 J/(g °C)).[46] Thus, all of the parameters in eq 28 can be measured or calculated except *z*, a coordination number. Chow evaluated 13 diluents in polystyrene and found that a value of 2 for *z* gave satisfactory fitting results.[61] This finding has been confirmed by other researchers for other polymer−diluent systems, such as CO_2 in PVC, polystyrene, polycarbonate, and PET,[57] and CO_2 in substituted polycarbonates,[65] even though in some systems, $z = 1$ might be more appropriate.[57] In this study, the calculated T_g values do not depend appreciably on *z* if it is 1 or 2, so in what follows, *z* is set to 2, consistent with Chow's original recommendation. In this sense, there are no adjustable parameters in eq 28. The following assumptions in Chow's model are of interest: (1) penetrant concentration must be low in the polymer and (2) the molar volume of the polymer repeat units should be comparable to that of the penetrant in the polymer.[61] The first assumption is valid in most cases of this study. The second assumption is valid for all penetrants except C_3H_6 and C_3H_8, which will be discussed later.

To provide an example of the magnitude of the T_g changes envisioned by the Chow model, Figure 10 presents the effect of penetrant concentration on the calculated T_g difference between the polymer/gas mixtures and the pure polymer for C_2H_4 and C_3H_6 at 273 K and for CO_2 at 273 and 253 K. The largest value of ($T_{g0} - T_g$), about 20 K, is observed for CO_2 at a concentration of about 70 cm^3(STP)/cm^3 polymer. Parts a−d of Figure 11 present the correlation between diffusion coefficients and fractional free volume. The lines are drawn based on eq 27, with A_D and *B* treated as adjustable constants for each penetrant. In general, this model describes the data for CO_2, CH_4, C_2H_6, and C_2H_4 adequately by using the values of A_D and *B* recorded in Table 5. This model requires two adjustable parameters (A_D and *B*) per penetrant to describe the temperature and pressure dependence of diffusivity, which represents a significant improvement over earlier approaches.[8,26,29] The results are satisfactory, considering that the diffusion coefficients for some of the gases vary by nearly 3 orders of magnitude. The model does not work as well for C_3H_8 and C_3H_6 as it does for the smaller gases. One possible reason could be an inaccurate estimate of the T_g change when C_3H_6 or C_3H_8 sorbs into XLPEGDA. The sorption of hydrocarbons such as C_3H_6 and C_3H_8 in polymers has not been modeled previously by using Chow's model. Potentially more importantly, the sizes of C_3H_6 and C_3H_8 (i.e., 73 and 80 cm^3/mole, respectively) are almost 100% larger than that of an ethylene oxide unit (i.e., 37 cm^3/mole), which violates one of the assumptions of Chow's model.[61]

Light gases, such as He, H_2, N_2, and O_2, typically have low solubility in polymers, and therefore, the change in T_g due to penetrant sorption can be neglected. This is a reasonable approximation because the sorption of CH_4, a more condensable (and, therefore, more soluble) penetrant than the light gases, does not affect the T_g of the system based on calculations using Chow's model. By assuming solubility is constant for light gases within the temperature range studied, eq 27 can be used to obtain the following expression for permeability:[53]

$$P_A = S_A D_A = S_A A_D \exp\left(\frac{-B}{FFV}\right) = A_P \exp\left(\frac{-B}{0.055 + 8.4 \times 10^{-4}(T - T_g)}\right) \quad (29)$$

where A_P is an adjustable constant. Figure 12 presents the fit of this equation to the experimental permeability coefficients of the light gases. The results are generally reasonable. The constants A_P and *B*, obtained by nonlinear least-squares fits of the data to eq 29, are recorded in Table 5. *B* values are also presented in Figure 13 for all penetrants as a function of Lennard−Jones diameter squared. In general, *B* values increase as penetrant size increases, which is qualitatively consistent with the original Cohen−Turnbull theory, which suggests that *B* should depend on the penetrant size.[49] The scaling with penetrant size squared is also reflected in the activated-state model (cf. Figure 7), and we return to this point later.

To summarize, the free volume model requires two parameters, A_D (or A_P) and *B*, to describe the effect of temperature and concentration on gas diffusivity or permeability. These two parameters can be evaluated by using gas diffusivity or permeability at two temperatures if the physical properties of the polymer, such as ΔC_{pp} and T_g, and gas sorption data (in cases where solubility depends significantly on temperature and/or pressure), are known. More elaborate free volume models are available,[66,67] but these are not widely used in modeling diffusion in gas separation membranes because of the large number of adjustable parameters required for their use.

Correspondence between the Activated Diffusion and Free Volume Models. The application of both activated diffusion[29] and free volume models to describe diffusion of small penetrants in rubbery XLPEGDA gives reasonable results, even though the physical basis of these two models are somewhat different. The activated diffusion model assumes that diffusion occurs only when a molecule has an energy that is higher than a threshold value (i.e., the activation energy of diffusion).[68] The free volume model views gas diffusion as the reorganization of free volume elements in the polymer near a molecule, with the diffusion step occurring when the free volume element is large enough to accommodate the penetrant molecule. There have been some efforts in the literature trying to correlate these two models quantitatively.[69,70] In this work, the correspondence between these approaches is further explored.

Combining eqs 12, 16, and 25 gives the following expression for the free volume model estimate of the effective

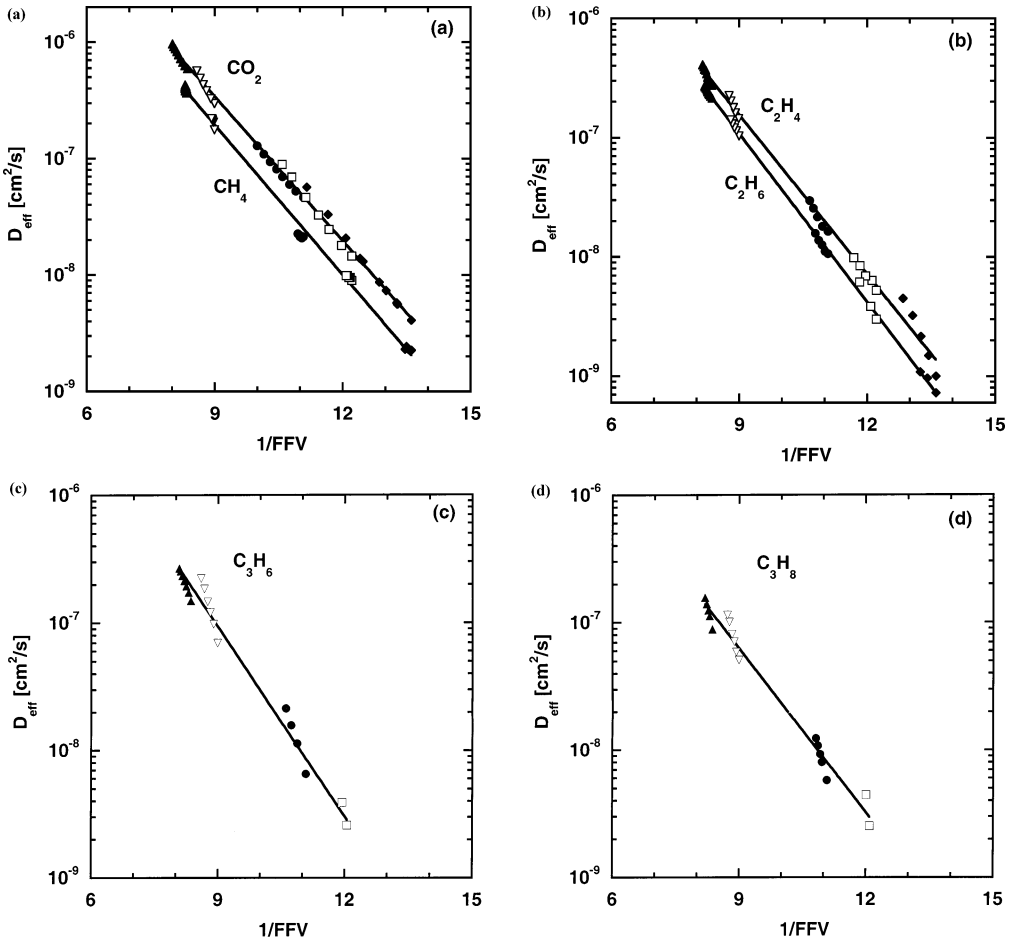

Figure 11. Correlation between fractional free volume of the polymer/penetrant mixtures and diffusion coefficients in XLPEGDA at various penetrant concentrations and temperatures: 308 K (▲), 298 K (▽), 273 K (●), 263 K (□), and 253 K (♦). (a) CO_2 and CH_4, (b) C_2H_6 and C_2H_4, (c) C_3H_6, (d) C_3H_8.

Table 5. Model Parameters for Diffusion Coefficients of CH_4, C_2H_4, CO_2, and C_2H_6, and for Permeability Coefficients of He, H_2, N_2, and O_2

penetrants	A_P ($\times 10^3$ Barrers)	B	A_D ($\times 10^{-3}$ cm^2/s)
He	4.0 ± 0.4	0.71 ± 0.01	
H_2	6.0 ± 0.6	0.72 ± 0.01	
N_2	7.3 ± 0.7	0.97 ± 0.02	
O_2	9.0 ± 0.9	0.89 ± 0.02	
CO_2		0.95 ± 0.02	1.8 ± 0.4
CH_4		0.99 ± 0.01	1.5 ± 0.3
C_2H_4		1.03 ± 0.02	1.7 ± 0.3
C_2H_6		1.08 ± 0.02	1.8 ± 0.4

activation energy of gas diffusion:

$$E_{D,F} = \frac{-B/FFV + (\ln A_D + b)}{a/R - 1/RT} \tag{30}$$

This equation suggests a linear correlation between E_D and B. Because E_D increases linearly with increasing d_{LJ}^2, as illustrated in Figure 7, B values should also be linearly related to d_{LJ}^2:

$$B = H + Ld_{LJ}^2 \tag{31}$$

where H and L are adjustable constants. Figure 13 presents a linear correlation between B values and d_{LJ}^2, which is consistent with eq 31.

On the basis of the activated-state model, the effective activation energy of diffusion ($E_{D,A}$) can be calculated from D_{eff} values by combining eqs 12 and 16 as follows:

$$E_{D,A} = \frac{\ln D_{eff} + b}{a/R - 1/RT} \tag{32}$$

$E_{D,A}$ and $E_{D,F}$ can be calculated as a function of temperature and penetrant concentration, and the results for various penetrants are presented in Figure 14. All of the data points are

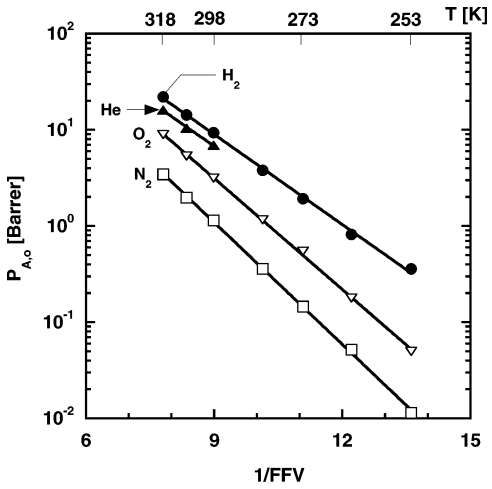

Figure 12. Correlation between fractional free volume of pure XLPEGDA and infinite dilution permeability coefficients of light gases in XLPEGDA at various temperatures.

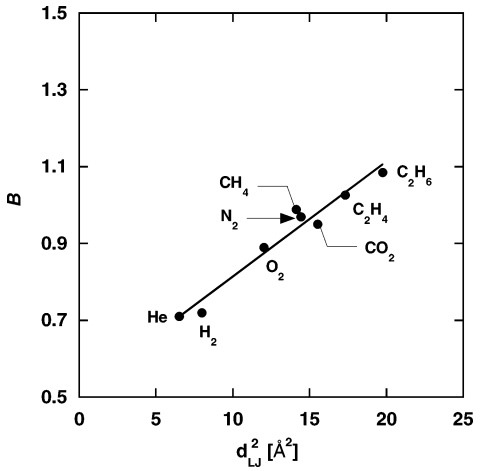

Figure 13. The dependence of B on penetrant Lennard−Jones diameter squared in XLPEGDA. The equation for the best fit line is $B = 0.51(\pm 0.02) + 0.030(\pm 0.002)\, d_{LJ}^2$ when the units of d_{LJ} are Å. The values of d_{LJ} are 2.55, 2.83, 3.47, and 3.80 Å for He, H_2, O_2, and N_2, respectively.[43] The d_{LJ} values for other penetrants are mentioned in the caption of Figure 7.

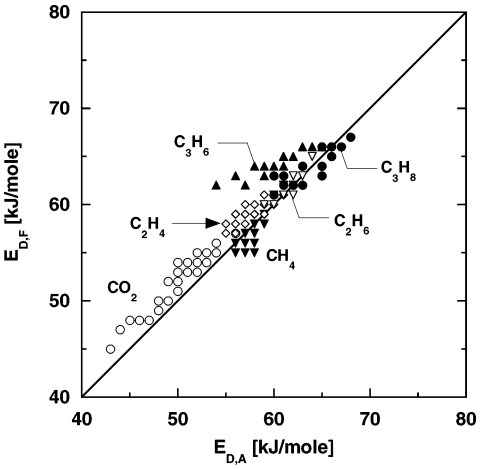

Figure 14. Comparison of activation energy of diffusion calculated based on the activated diffusion model ($E_{D,A}$) and the free volume model ($E_{D,F}$).

near the line of equality (which represents $E_{D,F} = E_{D,A}$), indicating consistency between the two models and the ability of both models to describe the experimental data. Under these circumstances, the free volume model and activated-state model of gas diffusion in polymers provide equivalent descriptions of the data. The activated-state model is exponential in $1/T$, while the free volume model is exponential in $1/FFV$, and FFV, in turn, is linear in T. It will be interesting to see if future theoretical and molecular modeling approaches validate and extend this interpretation.

Conclusions

In XLPEGDA, permeability increases as penetrant fugacity or concentration in the polymer increases for highly sorbing penetrants such as CO_2, C_2H_4, C_2H_6, C_3H_6, and C_3H_8, in large measure due to an increase in diffusivity with increasing concentration. Permeability to light gases (i.e., He, H_2, N_2, O_2, and CH_4) is independent of fugacity. As temperature increases, permeability and diffusivity for all penetrants increase, indicating positive values of E_p and E_D. Presumably because of its polar nature, XLPEGDA exhibits lower permeability coefficients and higher E_p and E_D values than nonpolar polymers such as natural rubber.

Two models (one based on activated diffusion and the other based on free volume) have been used to describe the temperature and concentration dependence of local effective diffusion coefficients. Both models describe the data reasonably well in most cases.

Acknowledgment. We gratefully acknowledge partial support of this work by the Chemical Sciences, Geosciences and Biosciences Division, Office of Basic Energy Sciences, Office of Science, U.S. Department of Energy (grant no. DE-FG03-02ER15362). This research work was also partially supported by the United States Department of Energy's National Energy Technology Laboratory under a subcontract from Research Triangle Institute through their prime contract no. DE-AC26-99FT40675. This work was also prepared with partial support from the U.S. Department of Energy, under award no. DE-FG26-01NT41280. However, any opinions, findings, conclusions, or recommendations expressed herein are those of the authors and do not necessarily reflect the views of the DOE. Partial support from the U.S. National Science Foundation under grant no. CTS-0515425 is also acknowledged.

References and Notes

(1) Baker, R. W. *Membrane Technology and Applications*, 2nd ed.; J. Wiley: New York, 2004.
(2) *Today's Hydrogen Production Industry*; http://www.fossil.energy.gov/programs/fuels/hydrogen/currenttechnology.shtml.
(3) Chiesa, P.; Consunni, S.; Kreutz, T.; Williams, R. *Int. J. Hydrogen Energy* **2005**, *30*, 747−767.
(4) Blume, I.; Pinnau, I. U.S. Patent 4,963,165, 1990.
(5) Bondar, V. I.; Freeman, B. D.; Pinnau, I. *J. Polym. Sci., Part B: Polym. Phys.* **1999**, *37*, 2463−2475.
(6) Bondar, V. I.; Freeman, B. D.; Pinnau, I. *J. Polym. Sci., Part B: Polym. Phys.* **2000**, *38*, 2051−2062.
(7) Okamoto, K.-i.; Fuji, M.; Okamyo, S.; Suzuki, H.; Tanaka, K.; Kita, H. *Macromolecules* **1995**, *28*, 6950−6956.
(8) Lin, H.; Freeman, B. D. *J. Membr. Sci.* **2004**, *239*, 105−117.
(9) Lin, H.; Freeman, B. D. *J. Mol. Struct.* **2005**, *739*, 57−74.
(10) Patel, N. P.; Miller, A. C.; Spontak, R. J. *Adv. Mater.* **2003**, *15*, 729−733.
(11) Hirayama, Y.; Kase, Y.; Tanihara, N.; Sumiyama, Y.; Kusuki, Y.; Haraya, K. *J. Membr. Sci.* **1999**, *160*, 87−99.
(12) Pinnau, I.; Freeman, B. D. *Polym. Mater. Sci. Eng.* **2002**, *86*, 108.
(13) Merkel, T. C.; Toy, L. G.; Coker, D. T.; Gupta, R. P.; Freeman, B. D.; Fleming, G. K. *Proc. Annu. Int. Pittsburgh Coal Conf.* **2002**, *19*, 713−723.
(14) Patel, N. P.; Miller, A. C.; Spontak, R. J. *Adv. Funct. Mater.* **2004**, *14*, 699−707.
(15) Chatterjee, G.; Houde, A. A.; Stern, S. A. *J. Membr. Sci.* **1997**, *135*, 99−106.
(16) Kim, J.; Ha, S.; Lee, Y. *J. Membr. Sci.* **2001**, *190*, 179−193.
(17) Metz, S. J.; Mulder, M. H. V.; Wessling, M. *Macromolecules* **2004**, *37*, 4590−4597.
(18) Lin, H.; Van Wagner, E.; Raharjo, R.; Freeman, B. D.; Roman, I. *Adv. Mater.* **2006**, *18*, 39−44.
(19) Lin, H.; Van Wagner, E.; Freeman, B. D.; Toy, L. G.; Gupta, R. P. *Science* **2006**, *311*, 639−642.
(20) Lin, H.; Kai, T.; Freeman, B. D.; Kalakkunnath, S.; Kalika, D. S. *Macromolecules* **2005**, *38*, 8381−8393.
(21) Lin, H.; Freeman, B. D. *Macromolecules* **2005**, *38*, 8394−8407.
(22) Petropoulos, J. H. In *Polymeric Gas Separation Membranes*; Paul, D. R., Yampolskii, Y. P., Eds.; CRC Press: Boca Raton, FL, 1994; pp 17−81.
(23) Freeman, B. D.; Pinnau, I. In *Polymer Membranes for Gas and Vapor Separation*; Freeman, B. D., Pinnau, I., Eds.; ACS Symposium Series 733; American Chemical Society: Washington DC, 1999; p 1.
(24) Schuld, N.; Wolf, B. A. In *Polymer Handbook*; Brandrup, J., Immergut, E. H., Grulke, E. A., Eds.; John Wiley & Sons: New York, 1999; pp VII-247−264.
(25) Koros, W. J.; Chan, A. H.; Paul, D. R. *J. Membr. Sci.* **1977**, *2*, 165−190.
(26) Stern, S. A.; Fang, S.-M.; Jobbins, R. M. *J. Macromol. Sci., Phys.* **1971**, *B5*, 41−70.
(27) Merkel, T. C.; Bondar, V. I.; Nagai, K.; Freeman, B. D.; Pinnau, I. *J. Polym. Sci., Part B: Polym. Phys.* **2000**, *38*, 415−434.

(28) Dixon-Garrett, S. V.; Nagai, K.; Freeman, B. D. *J. Polym. Sci., Part B: Polym. Phys.* **2000**, *38*, 1461−1473.
(29) Prabhakar, R. S.; Raharjo, R.; Toy, L. G.; Lin, H.; Freeman, B. D. *Ind. Eng. Chem. Res.* **2005**, *44*, 1547−1556.
(30) Felder, R. M.; Huvard, G. S. In *Methods of Experimental Physics*; Fava, R., Ed.; Academic Press.: New York, 1980; Vol. 16C, pp 315−377.
(31) Mogri, Z.; Paul, D. R. *J. Membr. Sci.* **2000**, *175*, 253−265.
(32) Lin, H.; Freeman, B. D. In *Springer Handbook of Materials Measurement Methods*; Czichos, H., Smith, L. E., Saito, T., Eds.; Springer Publishing: New York, 2006; release date June 2006.
(33) Crank, J. *The Mathematics of Diffusion*, 2nd ed.; Oxford University Press: New York, 1995.
(34) Bevington, P. R.; Robinson, D. K. *Data Reduction and Error Analysis for the Physical Sciences*, 2nd ed.; McGraw-Hill: New York, 1992.
(35) Koros, W. J.; Hellums, M. W. *Fluid Phase Equilib.* **1989**, *53*, 339−354.
(36) Singh, A.; Freeman, B. D.; Pinnau, I. *J. Polym. Sci., Part B: Polym. Phys.* **1998**, *36*, 289−301.
(37) Michaels, A. S.; Bixler, H. J. *J. Polym. Sci.* **1961**, *50*, 413−439.
(38) Michaels, A. S.; Bixler, H. J. *J. Polym. Sci.* **1961**, *50*, 393−412.
(39) Serad, G. E.; Freeman, B. D.; Stewart, M. E.; Hill, A. J. *Polymer* **2001**, *42*, 6929−6943.
(40) Dhoot, S. N.; Freeman, B. D.; Stewart, M. E.; Hill, A. J. *J. Polym. Sci., Part B: Polym. Phys.* **2001**, *39*, 1160−1172.
(41) Barbari, T. A.; Huang, C. H. *Abstracts of Papers*, 225th National Meeting of the American Chemical Society, New Orleans, LA, 2003; American Chemical Society, Washington, DC, 2003; POLY-419.
(42) Boyer, R. F. In *Encyclopedia of Polymer Science and Technology: Plastics, Resins, Rubbers, Fibers*; Bikales, N. M., Bickford, M., Eds.; John Wiley & Sons: New York, 1977; Vol. 2 (Supplement), pp 745−839.
(43) Poling, B. E.; Prausnitz, J. M.; O'Connell, J. P. *The Properties of Gases and Liquids*, 5th ed.; McGraw-Hill: New York, 2000.
(44) Merkel, T. C.; Bondar, V.; Nagai, K.; Freeman, B. D.; Yampolskii, Y. P. *Macromolecules* **1999**, *32*, 8427−8440.
(45) Freeman, B. D. *Macromolecules* **1999**, *32*, 375−380.
(46) Van Krevelen, D. W. *Properties of Polymers: Their Correlation with Chemical Structure: Their Numerical Estimation and Prediction from Additive Group Contributions*; Elsevier: Amsterdam, 1990.
(47) Meares, P. *J. Am. Chem. Soc.* **1954**, *76*, 3415−3422.
(48) Barrer, R. M.; Skirrow, G. *J. Polym. Sci.* **1948**, *3*, 549−563.
(49) Cohen, M. H.; Turnbull, D. *J. Chem. Phys.* **1959**, *31*, 1164−1169.
(50) Fujita, H. *Fortschr. Hochpolym. Forsch.* **1961**, *3*, 1−47.
(51) Vrentas, J. S.; Duda, J. L. *J. Polym. Sci., Part B: Polym. Phys. Ed.* **1977**, *15*, 403−16.
(52) Ganesh, K.; Nagarajan, R.; Duda, J. L. *Ind. Eng. Chem. Res.* **1992**, *31*, 746−755.
(53) Lee, W. M. *Polym. Eng. Sci.* **1980**, *20*, 65−69.
(54) Maeda, Y.; Paul, D. R. *J. Polym. Sci., Part B: Polym. Phys.* **1987**, *25*, 1005−1016.
(55) Zoller, P.; Walsh, D. *Standard Pressure−Volume−Temperature Data for Polymers*, 1st ed.; Technomic Publishing Co. Inc.: Lancaster, PA, 1995.
(56) Ismail, A. F.; Lorna, W. *Sep. Purif. Technol.* **2002**, *27*, 173−194.
(57) Chiou, J. S.; Barlow, J. W.; Paul, D. R. *J. Appl. Polym. Sci.* **1985**, *30*, 2633−2644.
(58) Condo, P. D.; Sanchez, I. C.; Panalotou, C. G.; Johnston, K. P. *Macromolecules* **1992**, *25*, 6119−6127.
(59) Wang, W. C.; Kramer, E. J.; Sachse, W. G. *J. Polym. Sci., Part B: Polym. Phys.* **1982**, *20*, 1371−84.
(60) Fried, J. R.; Liu, H.-C.; Zhang, C. *J. Polym. Sci., Part C: Polym. Lett. 27*, 385−92.
(61) Chow, T. S. *Macromolecules* **1980**, *13*, 362−364.
(62) Condo, P. D.; Paul, D. R.; Johnson, K. P. *Macromolecules* **1994**, *27*, 365−371.
(63) Dong, Z.; Fried, J. R. *Comput. Theor. Polym. Sci.* **1997**, *7*, 53−64.
(64) Martin, T. M.; Young, D. M. *Polymer* **2003**, *44*, 4747−4754.
(65) Banerjee, T.; Lipscomb, G. G. *J. Appl. Polym. Sci.* **1998**, *68*, 1441−1449.
(66) Vrentas, J. S.; Duda, J. L. *J. Polym. Sci., Part B: Polym. Phys.* **1977**, *15*, 417−439.
(67) Alsoy, S.; Duda, J. L. *AIChE J.* **1999**, *45*, 896−905.
(68) Kumins, C. A.; Kwei, T. K. In *Diffusion in Polymers*; Crank, J., Park, G. S., Eds.; Academic Press: New York, 1968; pp 107−140.
(69) Okamoto, K.; Tanaka, K.; Katsube, M.; Kita, H.; Sueoka, O.; Ito, Y. *Polym. J.* **1993**, *25*, 275−284.
(70) Yampolskii, Y. P.; Shishatskii, S.; Alentiev, A. Y.; Loza, K. *J. Membr. Sci.* **1998**, *148*, 59−69.
(71) van Amerongen, G. J. *J. Appl. Phys.* **1946**, *17*, 972−985.

MA051686O